THE JOURNAL OF PHYSICAL CHEMISTRY B

Article

pubs.acs.org/JPCB

Innovative Wavelet Protocols in Analyzing Elastic Incoherent Neutron Scattering

S. Magazù,* F. Migliardo, and M. T. Caccamo

Dipartimento di Fisica dell'Università degli Studi di Messina, Viale S. D'Alcontres 31, 98166, Messina, Italy

Supporting Information

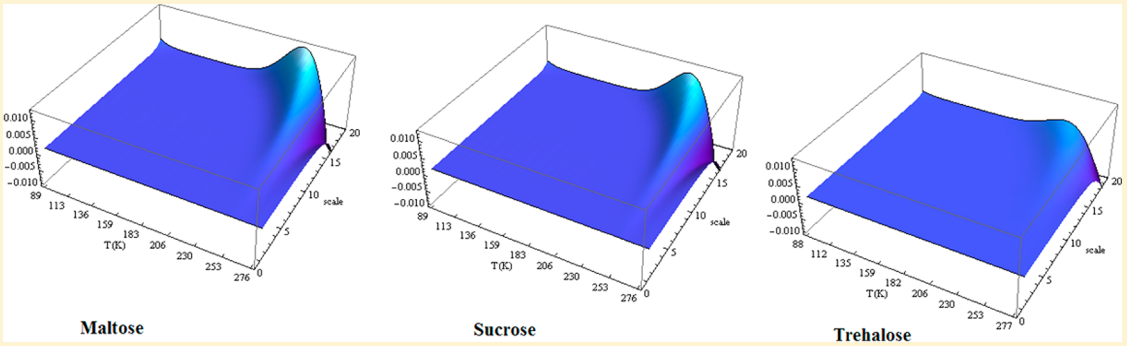

ABSTRACT: Wavelet analysis has recently found a wide range of applications in Physics, Mathematics, and signal processing. This is mainly due to its ability to locally resolve a nonstationary signal in terms of functional forms, called mother wavelets, and to firmly locate trend anomalies in the signal. In the present paper, some examples of the application of wavelet analysis to elastic incoherent neutron scattering (EINS) data collected by the IN13 spectrometer at the Institute Laue Langevin (ILL) on water mixtures of the three homologous disaccharides, trehalose, maltose, and sucrose, and on literature data of dry and hydrated lysozyme and myoglobine as a function of temperature and of exchanged wave vector are presented. The experimental findings have been analyzed by means of a wavelet analysis that allows one to characterize the scattered elastic intensity behavior on different scales and to locate the discontinuities and the trend anomalies in the registered signal. This latter procedure is made possible thanks to the multiscale analysis, which allows, by decreasing the scale, one to localize the peculiar trend features. The entire body of the experimental findings reveals different transition temperatures for the three investigated disaccharides together with a stronger temperature dependence of the maltose/H_2O and sucrose/H_2O systems in comparison with the trehalose/H_2O mixture, which signals a *stronger* character of this latter in comparison with the other two homologous disaccharides. These results justify the better ability of trehalose, with respect to maltose and sucrose, to encapsulate biostructures in a more rigid matrix.

I. INTRODUCTION

Recently, increasing attention has been given to clarify the molecular mechanisms responsible for the survival of many organisms under environmental stress conditions.[1] In particular, the term cryptobiosis, from the Greek *κριπτοσ* (i.e., hidden or coated), and bios (i.e., life) makes reference to the inactivated state occurring in some organisms when, in the occurrence of harsh environmental conditions, undetectable (hidden) levels of metabolic functions are reached.[2−4] Cryptobiotic organisms belong to all the natural kingdoms[5−7] encompassing many vegetal and animal species. In this frame, homologous disaccharides ($C_{12}H_{22}O_{11}$), e.g., trehalose, maltose, and sucrose, and in particular trehalose, have been shown to be cryptobiotic-activating substances, although the molecular mechanisms responsible for their bioprotectant effectiveness remain still cryptic.

The name trehalose derives from *Trehala manna*, the parasitic beetle whose cocoons contain manna or trehalose, which, according to legend, rained down in the desert after Moses's appeal to God (Exodus 16). The cocoons, found on thorn bushes, are highly nutritious consisting of 30% trehalose plus proteins and other substances.

Although many studies have been focused on ternary systems such as biostructures/water/bioprotectant molecules,[8−13] many researchers retain that the protein dynamics is strongly coupled with, and depends on, the solvent properties[14−23] and, for this reason, their attention has been addressed also to the water/bioprotectant molecules mixtures.

Within this framework, Green and Angell[8] suggested that the higher value of the glass transition temperature of trehalose and its mixtures with water, in comparison with the other disaccharides, is the only reason for its superior bioprotectant effectiveness; the higher T_g values of the trehalose/H_2O mixtures, with respect to the T_g values of the other

Received: June 19, 2012
Revised: July 12, 2012
Published: July 13, 2012

   dx.doi.org/10.1021/jp3060087 | J. Phys. Chem. B 2012, 116, 9417−9423

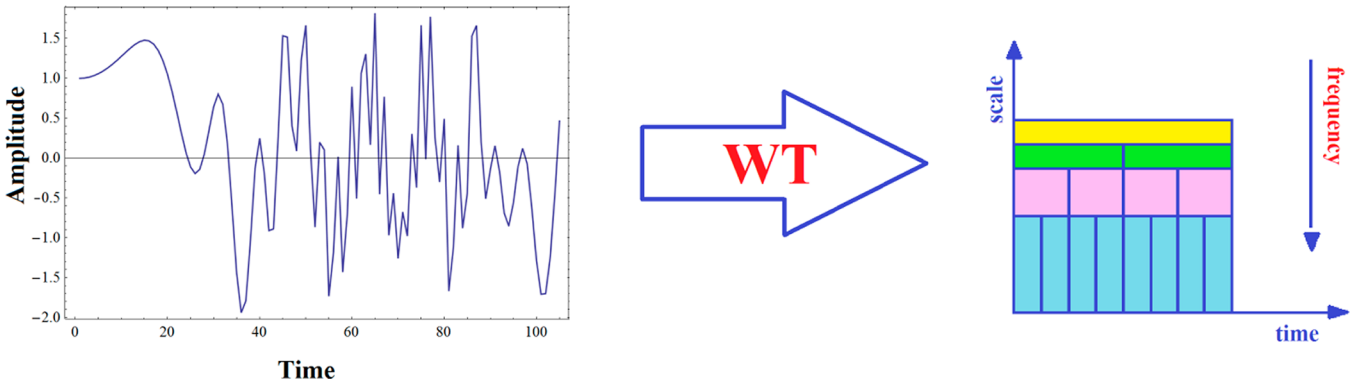

Figure 1. Using an MRA, it is possible to analyze a nonstationary signal at different frequencies with different resolutions. Every box corresponds to a value of the wavelet transform in the time−frequency plane. The wavelet analysis calculates the correlation between the signal under consideration and a wavelet function. The similarity between the signal and the analyzing wavelet function is computed separately for different time intervals, resulting in a 2D representation.

disaccharides/H_2O mixtures at all the concentration values, implies that, at a given temperature, the glass transition for trehalose mixtures always occurs at a higher water content, this property being important for bioprotection. However such a hypothesis alone is not fully satisfactory since other similar systems, such as, for example, dextran ($(C_6H_{10}O_5)x$),[17] a linear polysaccharide with $\alpha(1-6)$ glycosidic links, has an even higher T_g value, but do not show comparable bioprotective action.

On the other hand, Crowe et al.[2] hypothesized that a direct interaction between the sugars and the biostructures takes place; more specifically, they formulated the so-called "water-replacement hypothesis" for justifying the trehalose protective function through the existence of direct hydrogen bonding of trehalose with polar headgroups of the lipids, as water does.

Several experimental findings obtained by different spectroscopic investigations as well as some simulation studies[24−30] clearly indicate that the structural and the dynamical properties of water are drastically perturbed by disaccharides, and by trehalose with a greater extent. More specifically, neutron diffraction results[18,19] show for all disaccharides a strong distortion of the peaks linked to the hydrogen-bonded network in the partial radial distribution functions that can be attributed to the destroying of the tetrahedral coordination of pure water.[31−37] In addition Raman scattering findings[23] show that the addition of trehalose, with respect to the other disaccharides, destroys the tetrahedral intermolecular network of water, which gives rise to ice by a lowering of temperature. These results show that disaccharides have a noticeable kosmotropic character, namely that the disaccharide−water molecule interaction strength is higher with respect to that among the water molecules. Moreover, ultrasonic velocity measurements[22−24] put into evidence that, with respect to the other disaccharides, the trehalose−water system is characterized, in all the investigated concentration range, by both the highest value of the solute−solvent interaction strength and by the highest hydration number.

As far as dynamics is concerned, quasi elastic neutron scattering (QENS) results on disaccharide solutions[25] indicate that the water dynamics is strongly affected by the presence of disaccharides and by trehalose in particular. In addition, viscosity measurements on trehalose, maltose, and sucrose aqueous solutions[21] showed that trehalose has, with respect to the other disaccharides, a stronger kinetic character in Angell's classification scheme. QENS and inelastic neutron scattering (INS) were also employed to investigate the low frequency dynamics across the glass transition of trehalose, maltose, and sucrose water mixtures.[18−20] The obtained experimental findings, through the relaxational to the vibrational contribution ratio, confirm that the trehalose/H_2O mixture shows a stronger character.

Finally, a new operative definition for the degree of fragility of glass-forming systems has been furnished,[37] and, in this frame, the stronger character of the trehalose/H_2O mixture indicates a better ability with respect to maltose and sucrose/H_2O mixtures to encapsulate biostructures in a more rigid matrix.

Neutrons with a 1 Å wavelength and an energy close to 1 kcal/mol represent an excellent probe to characterize thermal molecular motions and conformational changes in biological systems.[38−44] In particular, they furnish information on mean-square fluctuations in a given time scale by elastic incoherent neutron scattering (EINS),[45] on correlation times of diffusion motions by QENS,[46] and on vibrational modes by INS.[47]

It is also well-known that, in comparison with QENS, EINS, due to the fact that the elastic contribution is often a factor of 100−1000 higher than the quasi-elastic one at low energy transfer, requires a relatively small amount of material; this point allows the investigation of a relevant number of interesting systems, such as, for example, those of interest in the biophysical field. Furthermore when dealing with QENS, one of the main drawbacks is constituted by the relatively high number of fitting parameters. In this frame, EINS, through the so-called "elastic window method" is one of the most effective approaches for evaluating atomic mean square displacement (MSD) in hydrogenous systems, and it is often preferred to the QENS technique.[47−49] The MSDs obtained by an analysis as a function of Q are dominated by hydrogen motions due to its large incoherent cross-section value.[47−49]

In this work, EINS intensity results on homologous disaccharide (trehalose, maltose, and sucrose)/H_2O mixtures as a function of concentration and temperature and on literature data of hydrated lysozyme and myoglobine[41,43] are analyzed by means of a wavelet analysis.

It is well-known that wavelet analysis makes it possible to locally resolve a nonstationary signal in terms of functional forms called mother wavelets and to carefully locate anomalies in the signal. In particular, it allows a time/frequency characterization of a signal, similar to a musical score, which furnishes a representation of music in terms of both note order and frequency length.

dx.doi.org/10.1021/jp3060087 | J. Phys. Chem. B 2012, 116, 9417−9423

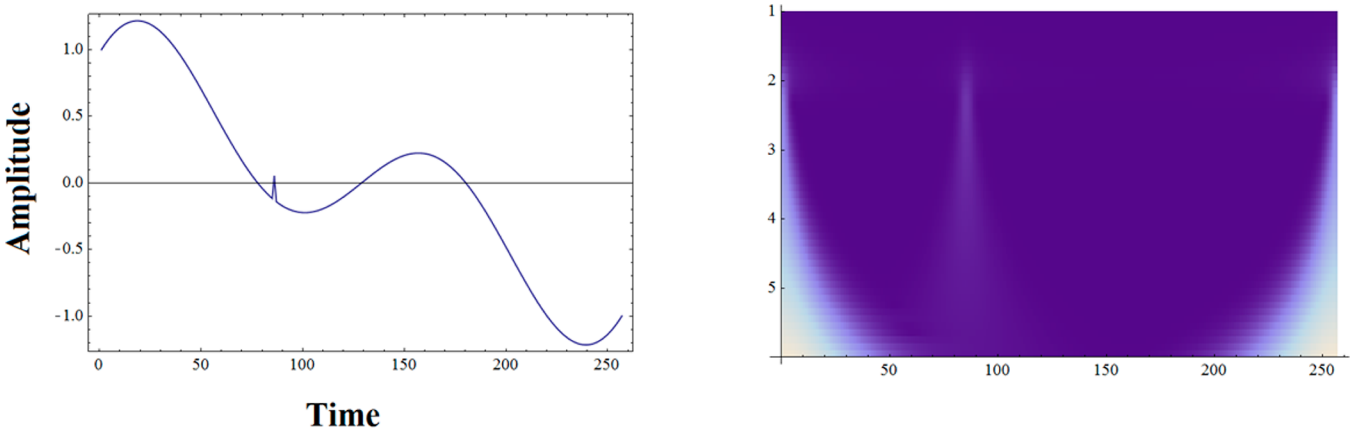

Figure 2. A signal with a sudden spike (on the left) and its 2D scalogram plot (on the right). The wavelet transform, which defines a local time−frequency energy density, clearly reveals the spike of the signal.

In analyzing the thermal behavior of both the elastically scattered intensity in EINS as well as of MSD, one has to face the characterization of the behavior global features and the objective identification of the temperature values for which "kinks" and/or anomalies in the trends occur. In this frame, the wavelet analysis proves to be a powerful tool since it allows a multiscale study, which makes possible both such a global characterization as well as the trend anomalies localization. The latter is made possible thanks to the wavelet multiscale analysis, which allows, by decreasing the scale, one to evaluate the trend features localization.

In this paper, the wavelet analysis of EINS data allows one to (i) put into evidence the differences in the spectral features of the three homologous disaccharides showing smaller spectral changes induced by temperature for trehalose in comparison with maltose and sucrose; this indicates a better ability of trehalose with respect to maltose and sucrose to encapsulate biostructures in a more rigid matrix; and (ii) carefully localize the transitions in the EINS and MSD versus T behavior for the three disaccharides, for hydrated lysozyme, and for myoglobine.[41,43]

II. WAVELET ANALYSIS

Wavelet analysis is a powerful tool in signal processing. Most signals contain numerous nonstationary or transitory characteristics: drift, trends, abrupt changes, and beginnings and ends of events; wavelet analysis allows the use of long time intervals where one wants more precise low-frequency information, and shorter regions where one wants high-frequency information. It does not use a time frequency region, but rather a time-scale region. The major advantage offered by wavelets is the ability to perform local analysis, that is, to analyze a localized area of a larger signal.

In Figure 1, it is shown how, using an approach called multiresolution analysis (MRA), it is possible to analyze a nonstationary signal at different frequencies with different resolutions. Every box corresponds to a value of the wavelet transform in the time-frequency plane. It should be noticed that boxes have a certain nonzero area, which implies that the value of a particular point in the time-frequency plane cannot be known. All the points in the time-frequency plane that fall into a box are represented by one value of the wavelet transform. The first thing to notice is that, although the widths and heights of the boxes change, the area is constant; in other words, each box represents an equal portion of the time-frequency plane, but giving different proportions to time and frequency. In addition, at low frequencies, the heights of the boxes are shorter (which corresponds to better frequency resolutions, since there is less ambiguity regarding the value of the exact frequency), but their widths are longer (which correspond to a poor time resolution, since there is more ambiguity regarding the value of the exact time). At higher frequencies, the width of the boxes decreases, i.e., the time resolution gets better, and the heights of the boxes increase, i.e., the frequency resolution gets poorer.

Wavelet analysis is capable of revealing aspects of data that other signal analysis techniques miss: e.g., aspects such as trends, discontinuities in higher derivatives, and self-similarity features. Furthermore, because it allows a different view of data than those presented by other traditional techniques, wavelet analysis can often compress or denoise a signal without appreciable degradation.[50,51]

In Figure 2 a signal with a sudden spike is shown; the wavelet analysis, which defines a local time−frequency energy density, clearly reveals the spike of the signal.

It should be noticed that wavelet analysis is the breaking up of a signal into shifted and scaled versions of the mother wavelet, and that local features can be better described with wavelets that have the same local extent.

In Figure 3, on the top, it is shown how the mother wavelet changes with the scale parameter s. If $s < 1$, the wavelet function is contracted; in such case of relatively low scale, the frequency is relatively high, and there is a nondetailed global view of the signal. On the other hand, if $s < 1$, the wavelet is expanded, the scale is high, and the frequency is low. Additionally, the shifting of a wavelet simply consists of delaying or anticipating its time position.

Let L^2 ($\mathbb{R}$) denote the space of Lebesgue measurable functions. Let $\psi(t) \in L^2$ ($\mathbb{R}$) be a fixed function. The function $\psi(t)$ is said to be a wavelet if it satisfies

(i) finite energy

$$E = \int_{-\infty}^{\infty} |\psi(t)|^2 \, dt < \infty \tag{1}$$

(ii) admissibility condition

$$C_\Psi = \int_0^{\infty} \frac{|\hat{\psi}(\omega)|^2}{|\omega|} \, d\omega < \infty \tag{2}$$

where $\hat{\psi}$ denotes the Fourier Transform of $\psi(t)$, and

(iii) zero average

dx.doi.org/10.1021/jp3060087 | J. Phys. Chem. B 2012, 116, 9417−9423

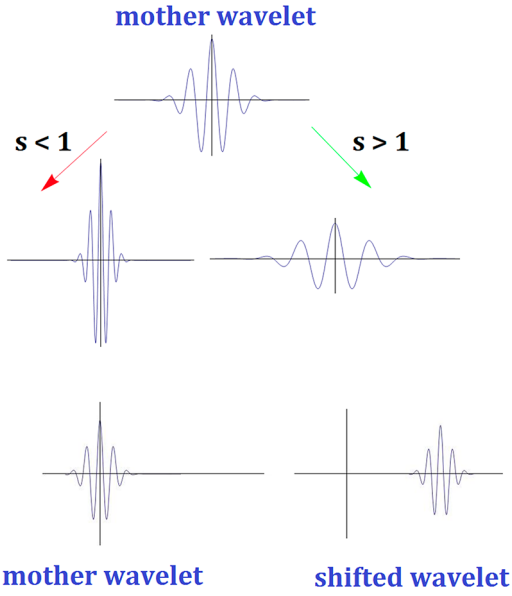

Figure 3. Wavelet changes with the variation of the scaling and of the shifting parameters.

$$\int_{-\infty}^{\infty} \psi(t)\, dt = \hat{\psi}(0) = 0 \tag{3}$$

An analytic wavelet transform allows one to calculate wavelet coefficients, and it defines a local time−frequency energy density called *scalogram* denoted by

$$P_{W_y}(\tau, s) = |W_y(\tau, s)|^2 \tag{4}$$

The latter provides the energy evolution with time in a single process by viewing a map of the square of the wavelet coefficients, and it has the advantage of revealing pockets of high and low energy on a different frequency basis.

In Figure 4, a nonstationary signal together with its two-dimensional (2D) scalogram and its three-dimensional (3D) scalogram of wavelet's coefficients are shown. In the 2D scalogram, the *x*-axis shows the time of observation and the *y*-axis shows the factor scale. The intensity of the color indicates the magnitude of the coefficient of the wavelet; lighter colors correspond to larger coefficients. The graph also provides the position (in time or in space) of the various frequencies. In the 3D scalogram, the *z*-axis gives the wavelet coefficients.

III. EXPERIMENTAL SECTION

EINS experiments were performed by using the IN13 spectrometer at the Institute Laue Langevin (ILL) in Grenoble, France. The relatively high energy of the incident neutrons (16 meV) allows one to span a wide range of momentum transfer Q ($\lesssim$5.5 Å^{-1}) with a very good energy resolution (full width at half maximum (fwhm) $\sim$ 8 μeV). In the used IN13 configuration, the incident wavelength was 2.23 Å and the Q-range was 0.28−4.27 Å^{-1}. Raw data were corrected for cell scattering and detector response and normalized to unity at Q = 0 Å^{-1}. Ultrapure powdered trehalose, maltose, and sucrose, and H_2O, purchased by Aldrich-Chemie (Milan, Italy), were used for the experiments. Measurements were performed in the temperature range of 20−310 K on hydrogenated trehalose, maltose, and sucrose in H_2O and on partially deuterated trehalose, maltose, and sucrose in D_2O at a weight-fraction value corresponding to 19 water (H_2O and D_2O) molecules for each disaccharide molecule. EINS and MSD data on hydrated myoglobine and lysozyme have been taken from the literature.[41,43]

IV. RESULTS AND DISCUSSION

In Figure 5, a comparison among EINS spectra of sucrose+19 H_2O (a), maltose+19 H_2O (b), and trehalose+19 H_2O (c) mixtures is shown.

In the second and third row, the approximation coefficients (second row) and the detail coefficients (third row) resulting from the Haar wavelet analysis are shown. It clearly appears that sucrose and maltose, in comparison with the other disaccharide, i.e., trehalose, reveal the most pronounced spectral changes, showing a higher sensitivity to temperature changes. These results confirm the lower fragile character of trehalose and indicate a better ability with respect to maltose and sucrose to encapsulate biostructures in a more rigid matrix.

In the last row (fourth row), the 3D scalograms, obtained by a wavelet analysis for EINS spectra as a function of temperature, on sucrose (a), maltose (b), and trehalose (c) water mixtures are reported. It is evident that the 3D scalograms reveal the presence of a transition for the trehalose/H_2O mixture at $T \sim 238$ K, and for maltose/H_2O and sucrose/H_2O mixtures at $T \sim 156$ K and $T \sim 233$ K, respectively.

Figure 6 shows the temperature dependence of the EINS intensity (binned over the total explored Q range) versus temperature for myoglobine (data taken from ref 41); the wavelet analysis allows one to detect and represent the relevant transitions as sharp changes in the scalogram and has the

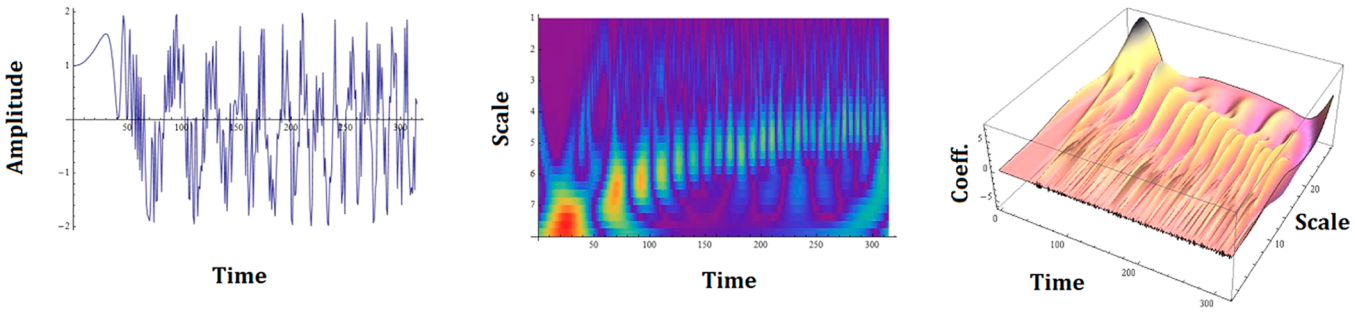

Figure 4. Nonstationary signal (on the left) together with its 2D scalogram (in the center) and its 3D scalogram (on the right). 2D scalogram: the *x*-axis gives the observation time, while the *y*-axis gives the coefficient scale. A pixel's color is associated, at a fixed location and scale, with the coefficient amplitudes. 3D scalogram: the *x*-axis gives the observation time, the *y*-axis gives the coefficient scale, and the *z*-axis gives the wavelet coefficients.

dx.doi.org/10.1021/jp3060087 | J. Phys. Chem. B 2012, 116, 9417−9423

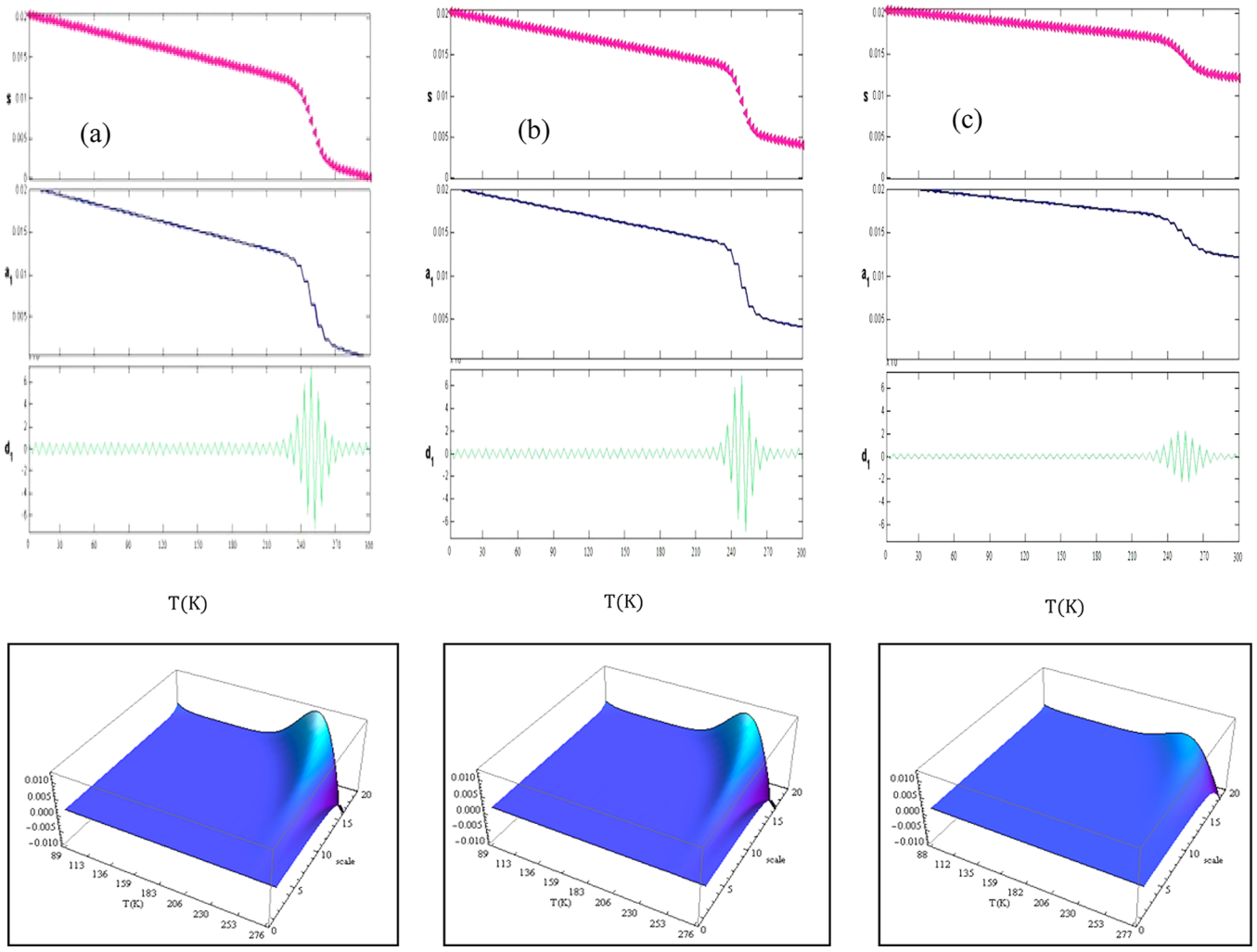

Figure 5. EINS profiles for sucrose+19 H_2O (a), maltose+19 H_2O (b), and trehalose+19 H_2O mixtures (c) as a function of temperature, together with the approximation (second row) and the detail coefficient (third row) profiles resulting from the wavelet analysis. The *x*-axis of three rows gives the temperature values in Kelvin. It clearly emerges that trehalose in comparison with the other two homologous disaccharides, i.e., sucrose and maltose, shows less pronounced spectral changes, revealing a lower sensitivity to temperature changes. These results, which confirm the lower fragile character of trehalose, justify its better bioprotective effectiveness. Last row: 3D scalograms obtained by wavelet analysis for EINS spectra as a function of temperature for sucrose, maltose, and trehalose water mixtures (i.e.: 1 disaccharide/19 water molecules).

advantage of being model-independent: myoglobine undergoes two transitions, one at $T \sim 156$ *K*, and the other at $T \sim 230$ *K*.

In Figure 7, the temperature dependence of the MSD, $\langle u^2(T)\rangle$ for the trehalose+19H_2O mixture is reported. As it can be seen, a mild transition is registered at $T \sim 238$ K; the relative 3D scalogram shows two kinks: one at $T \sim 238$ K and the other at $T \sim 254$ K.

In order to report further examples of wavelet analysis, in Figure 8 the behavior of $\langle u^2(T)\rangle_{tot}$ as a function of temperature for lysozyme in deuterated glucose at $h = 0$ is reported (data taken from ref 43); over the temperature range, the relative scalogram exhibits two main breaks: one at $T \sim 306$ K, and the other at $T \sim 372$ K. Finally, in figure 9, the MSD, $\langle u^2(T)\rangle_{tot}$, versus temperature for D_2O hydrated lysozyme/glycerol (50:50) for hydration values $h = 0.1$ is reported (data taken from ref 43); the 3D scalogram obtained by wavelet analysis shows a kink at $T \sim 233$ K.

V. CONCLUSIONS

One of the most debated points in analyzing the behavior of some physical observables, such as the EINS intensity and the MSD, lies in the determination of the transition temperature value for which a kink or an anomaly is registered in the spectrum profile. Such a determination, in fact, suffers great indetermination since it can be performed by following many different protocols. Just to report an example, the protein dynamical transition is usually referred to as a kink in the MSD observed in hydrated proteins with respect to the dry sample; then, the temperature value of this kink is registered by assuming an Einstein−Debye behavior at the lowest temperature values, while the temperature value relative to the deviation from such quasi-linear behavior is assumed as the kink temperature. It is therefore important to determine an objective protocol able to localize such a kink. In this framework, the wavelet analysis proves to be a striking tool for highlighting all the behavior anomalies.

In the present paper, some examples of the application of wavelet analysis to EINS data collected on water mixtures of the three homologous disaccharides, trehalose, maltose, and sucrose, and on literature data of dry and hydrated lysozyme and myoglobine are presented. The experimental findings have been analyzed by means of a wavelet analysis that allows one to

dx.doi.org/10.1021/jp3060087 | *J. Phys. Chem. B* 2012, 116, 9417−9423

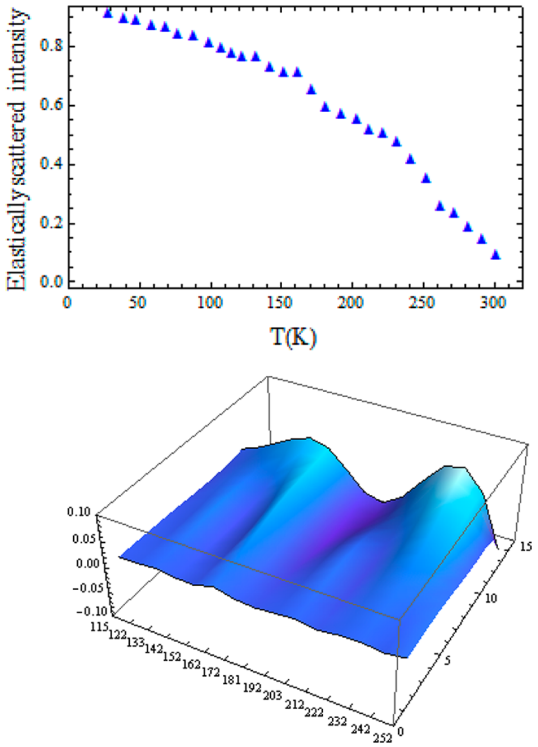

Figure 6. Elastically scattered intensity, binned over the explored Q range, as a function of temperature for hydrated powders (h = 0.2) of myoglobine on the top (data taken from ref 41); on the bottom, its relative 3D scalogram, obtained by the wavelet transform of EINS versus T spectrum, which reveals two transitions at $T \sim 156$ K and at $T \sim 230$ K.

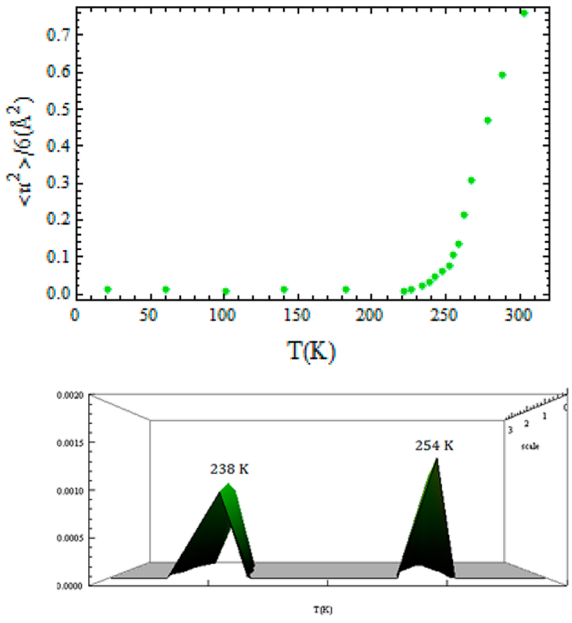

Figure 7. MSD temperature dependence for trehalose+19H_2O, which reveals a mild transition at ~238 K; the relative 3D scalogram, obtained by wavelet transform, reveals two kinks at $T \sim 238$ K and at $T \sim 254$ K .

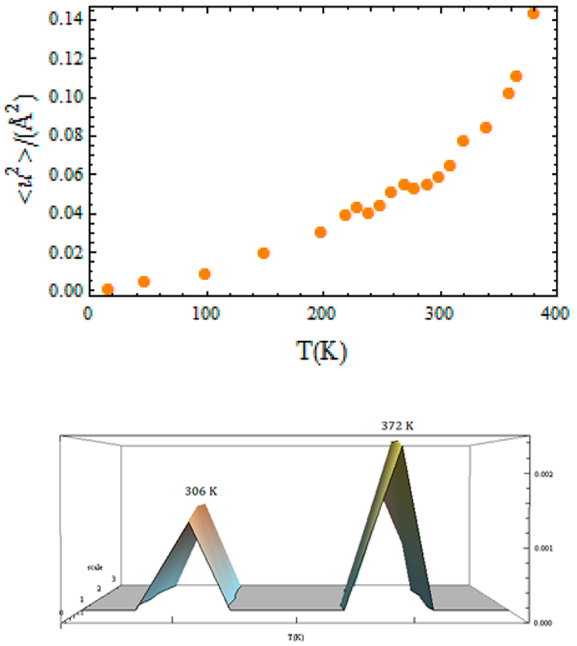

Figure 8. MSD as a function of temperature for lysozyme in deuterated glucose at h = 0 (data taken from ref 43); the wavelet analysis allows one to identify the crossover temperature values at $T \sim$ 306 K and at $T \sim$ 372 K.

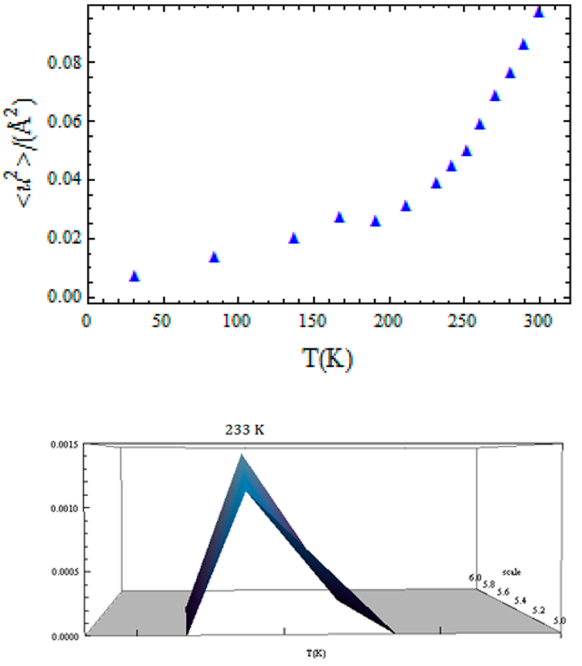

Figure 9. MSD as a function of temperature for D_2O hydrated lysozyme/glycerol (50:50) for h = 0.1 on the top (data taken from ref 43) and its relative 3D scalogram, which shows a kink at $T \sim$ 233 K.

characterize the scattered elastic intensity behavior on different scales and to locate the trend anomalies. The analysis reveals different transition temperatures for the three investigated disaccharides and a stronger temperature dependence of the maltose/H_2O and sucrose/H_2O systems in comparison with the trehalose/H_2O mixture, which signals a "stronger" character of this latter. These results justify the better ability of trehalose to encapsulate biostructures in a more rigid matrix.

dx.doi.org/10.1021/jp3060087 | J. Phys. Chem. B 2012, 116, 9417–9423

■ ASSOCIATED CONTENT

Supporting Information

Details of the continuous wavelet transform and the discrete wavelet transform. This information is available free of charge via the Internet at http://pubs.acs.org.

■ AUTHOR INFORMATION

Corresponding Author

*E-mail: smagazu@unime.it.

Notes

The authors declare no competing financial interest.

■ REFERENCES

(1) Crowe, J. H.; Crowe, L. M. *Science* **1984**, *223*, 701−703.
(2) Crowe, J. H.; Cooper, A. F., Jr. *Sci. Am.* **1971**, *225*, 30−36.
(3) Hirsh, A. *Cryobiology* **1987**, *24*, 214−228.
(4) Storey, K. B.; Storey, J. M. *Annu. Rev. Physiol.* **1992**, *54*, 619−637.
(5) Lee, R. E., Jr.; Costanzo, J. P.; Davidson, E. C.; Layne, J. R., Jr. *J. Therm. Biol.* **1992**, *17*, 263−266.
(6) Miller, L. K. *Comp. Biochem. Physiol.* **1978**, *59A*, 327−334.
(7) Zentella, R.; Mascorro-Gallardo, J. O.; Van Dijck, P.; Folch-Mallol, J.; Bonini, B.; Van Vaeck, C.; Gaxiola, R.; Covarrubias, A. A.; Nieto-Sotelo, J.; Thevelein, J. M.; Iturriaga, G. *Plant Physiol.* **1999**, *119*, 1473−1482.
(8) Green, J. L.; Angell, C. A. *J. Phys. Chem. B* **1989**, *93*, 2880−2882.
(9) Crowe, J. H.; Clegg, J. S.; Crowe, L. M. Anhydrobiosis: The Water Replacement Hypothesis. In *The Roles of Water in Foods*; Chapman & Hall: New York, 1998.
(10) Donnamaria, M. C.; Howard, E. I.; Grigera, J. R. *J. Chem. Soc., Faraday Trans.* **1994**, *90*, 2731−2735.
(11) Cordone, L.; Galajda, P; Vitrano, E.; Gassman, A.; Ostermann, A.; Parak, F. *Biophys. J.* **1998**, *27*, 173−176.
(12) Cordone, L.; Ferrand, M.; Vitrano, E.; Zaccai, G. *Biophys. J.* **1999**, *76*, 1043−1047.
(13) Cottone, G.; Cordone, L.; Ciccotti, G. *Biophys. J.* **2001**, *80*, 931−938.
(14) Paciaroni, A.; Cinelli, S.; Onori, G. *Biophys. J.* **2002**, *83*, 1157−1164.
(15) Frauenfelder, H.; Sligar, S. G.; Wolynes, P. G. *Science* **1991**, *254*, 1598−1603.
(16) Frauenfelder, H.; McMahon, B. *Proc. Natl. Acad. Sci. U.S.A.* **1998**, *9995*, 4795−4797.
(17) Oliver, A. E.; Crowe, L. M.; Crowe, J. H. *Seed Sci. Res.* **1998**, *8*, 211−221.
(18) Branca, C.; Magazù, S.; Migliardo, F. *Recent Res. Dev. Phys. Chem.* **2002**, *6*, 35−73.
(19) Branca, C.; Magazù, S.; Maisano, G.; Migliardo, F.; Romeo, G. *Philos. Mag. B* **2002**, *82*, 347−355.
(20) Branca, C.; Magazù, S.; Maisano, G.; Migliardo, F. *Phys. Rev. B* **2001**, *64*, 2242041−2242048.
(21) Branca, C.; Magazù, S.; Maisano, G.; Migliardo, F.; Romeo, G. *J. Phys. Chem. B* **2001**, *105*, 10140−10145.
(22) Branca, C.; Faraone, A.; Magazù, S.; Maisano, G.; Migliardo, F.; Migliardo, P.; Villari, V. *Recent Res. Dev. Phys. Chem.* **1999**, *3*, 361−403.
(23) Branca, C.; Magazù, S.; Maisano, G.; Migliardo, P. *J. Chem. Phys.* **1999**, *111*, 281−287.
(24) Magazù, S.; Migliardo, P.; Musolino, A. M.; Sciortino, M. T. *J. Phys. Chem. B* **1997**, *101*, 2348−2351.
(25) Magazù, S.; Villari, V.; Migliardo, P.; Maisano, G.; Telling, M. T. F. *J. Phys. Chem. B* **2001**, *105*, 1851−1855.
(26) Magazù, S.; Migliardo, F.; Mondelli, C.; Vadalà, M. *Carbohydr. Res.* **2005**, *340*, 2796−2801.
(27) Magazù, S.; Maisano, G.; Migliardo, P.; Tettamanti, E; Villari, V. *Mol. Phys.* **1999**, *96*, 381−387.
(28) Magazù, S.; Maisano, G.; Migliardo, P.; Villari, V. *J. Chem. Phys.* **1999**, *111*, 9086−9092.
(29) Ballone, P.; Marchi, M.; Branca, C.; Magazù, S. *J. Phys. Chem. B* **2000**, *104*, 6313−6317.
(30) Magazù, S.; Migliardo, F.; Telling, M. T. F. *J. Phys. Chem. B* **2006**, *110*, 1020−1025.
(31) Crupi, V.; Jannelli, M. P.; Magazù, S.; Maisano, G; Majolino, D; Migliardo, P.; Ponterio, R. *J. Mol. Struct.* **1996**, *381*, 207−212.
(32) Magazù, S.; Migliardo, F.; Benedetto, A. *J. Phys. Chem. B* **2011**, *115*, 7736−7743.
(33) Branca, C.; Magazù, S.; Maisano, G.; Migliardo, F.; Migliardo, P.; Romeo, G. *J. Chem. Phys.* **2002**, *106*, 10272−10276.
(34) Faraone, A; Magazù, S.; Maisano, G.; Ponterio, R.; Villari, V. *Macromolecules* **1999**, *32*, 1128−1133.
(35) Magazù, S.; Migliardo, F.; Ramirez-Cuesta, A. J. *J. R. Soc. Interface* **2005**, *2*, 527−532.
(36) Magazù, S. *Phys. B* **1996**, *26*, 92−106.
(37) Magazù, S.; Maisano, G.; Migliardo, F.; Mondelli, C. *Biophys. J.* **2004**, *86*, 3241−3249.
(38) Frauenfelder, H.; Chen, G.; Berendzen, J.; Fenimore, P. W.; Jansson, H.; McMahon, B. H.; Stroec, I. R.; Swenson, J.; Young, R. D. *Proc. Natl. Acad. Sci. U.S.A.* **2009**, *106*, 5129−5134.
(39) Lusceac, S. A.; Vogel, M. *J. Phys. Chem. B* **2010**, *114*, 10209−10216.
(40) Fu, L.; Villette, S.; Petoud, S.; Fernandez-Alonso, F.; Saboungi, M. L. *J. Phys. Chem.* **2011**, *115*, 1881−1888.
(41) Schirò, G.; Caronna, C.; Natali, F.; Cupane, A. *J. Am. Chem. Soc.* **2010**, *132*, 1371−1376.
(42) Khodadadi, S.; Curtis, J E.; Sokolov, A. P *J. Phys. Chem. B* **2011**, *115*, 6222−6226.
(43) Capaccioli, S.; Ngai, K. L.; Ancherbak, S.; Paciaroni, A. *J. Phys. Chem. B* **2012**, *116*, 1745−1757.
(44) Magazù, S.; Migliardo, F.; Benedetto, A. *J. Phys. Chem. B* **2010**, *114*, 9268−9274.
(45) Zaccai, G. *Science* **2000**, *288*, 1604−1607.
(46) Doster, W.; Cusack, S.; Petry, W. *Nature* **1989**, *337*, 754−756.
(47) Smith, J. C. *Q. Rev. Biophys.* **1991**, *24*, 227−291.
(48) Bicout, D. J.; Zaccai, G. *Biophys. J.* **2001**, *80*, 1115−1123.
(49) Réat, V.; Dunn, R.; Ferrand, M.; Finney, J. L.; Daniel, R. M.; Smith, J. C. *Proc. Natl. Acad. Sci. U.S.A.* **2000**, *97*, 9961−9966.
(50) Van Den Berg, J. C. *Wavelet in Physics*; Cambridge University Press: Cambridge, 1999.
(51) Mallat, S. G. *IEEE Trans. Pattern Anal. Machine Intell.* **1989**, *2*, 674−682.